Angewandte Chemie
Eine Zeitschrift der Gesellschaft Deutscher Chemiker

Supporting Information

Development of High Energy Density Diaminocyclopropenium-Phenothiazine Hybrid Catholytes for Non-Aqueous Redox Flow Batteries

*Yichao Yan, David B. Vogt, Thomas P. Vaid, Matthew S. Sigman, and Melanie S. Sanford**

ange_202111939_sm_miscellaneous_information.pdf

I. Synthetic Procedures

General Information. All commercial chemicals were used as received unless stated otherwise. Anhydrous CH_2Cl_2 was obtained from an Innovative Technology (now rebranded to Inert) solvent purification system. Reactions were performed under a nitrogen atmosphere. 3,7-Dimethoxy-10H-phenothiazine was prepared according to a reported method.[1] Compound **5** was prepared as the tosylate salt using a published method[2] and was then subjected to anion-exchange with NH_4PF_6. 1-Chloro-2,3-bis(dialkylamino)cyclopropenium chloride was prepared according to a literature procedure.[3,4] NMR spectra were obtained on Varian VNMRs 700, Varian VNMRs 500, Varian Inova 500, or Varian MR400 spectrometers. ^1H and ^{13}C chemical shifts are reported in parts per million (ppm) relative to TMS, with the residual solvent peak used as an internal reference. High resolution mass spectroscopy (HRMS) was performed on a Micromass AutoSpec Ultima Magnetic Sector Mass Spectrometer using electrospray ionization (ESI).

General procedure for the synthesis of 3 and 4. Under a N_2 atmosphere, the appropriate phenothiazine derivative (0.18 mmol, 1 equiv) was dissolved in dry THF (2 mL). Sodium hydride (0.22 mmol, 1.2 equiv) was added at room temperature. After stirring for 1 h, 1-chloro-2,3-bis(dialkylamino)cyclopropenium chloride (0.18 mmol, 1 equiv) was added. The mixture was then heated at 50 °C for overnight. The reaction was quenched with 1 M HCl (10 mL), and the resulting solution was extracted with dichloromethane (3 x 20 mL). The organic extracted were collected and concentrated under reduced pressure. The resulting residue was dissolved in water (5 mL), and ammonium hexafluorophosphate (2 equiv) was added with vigorous stirring. A precipitate formed, and this material was extracted into CH_2Cl_2 (3 × 15 mL). The combined organic extractys were dried over Na_2SO_4 and concentrated under reduced pressure. Column chromatography on silica gel afforded **3** and **4**.

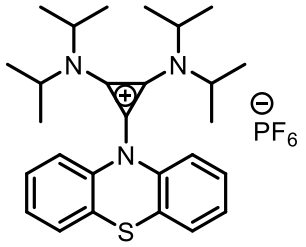

Synthesis of 3-*i*Pr: The general procedure was followed using 1-chloro-2,3-bis(diisopropylamino)cyclopropenium chloride[3,5] as the substrate. Compound **3-*i*Pr** was isolated as a white powder (11 mg, 18% yield) using 5% ethyl acetate in DCM as the eluent. R_F = 0.26 in 5% ethyl acetate/ DCM. ^{1}H NMR (500 MHz, CD_3CN) δ 7.19-7.08 (multiple peaks, 4H), 7.08-6.97 (m, 2H), 6.83-6.70 (m, 2H), 4.03 (hept, *J* = 6.8 Hz, 4H), 1.30 (d, *J* = 6.8 Hz, 24H).^{13}C NMR (126 MHz, CD_3CN) δ 138.55, 136.16, 128.49, 128.18, 125.94, 120.92, 117.45, 102.89, 53.98, 21.80. HRMS (ESI) *m/z* calcd for $C_{27}H_{36}N_3S^+$ (**3-*i*Pr**$^+$): 434.2624, found: 434.2619.

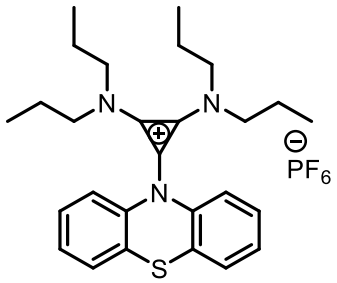

Synthesis of 3-*n*Pr: The general procedure was followed using 1-chloro-2,3-bis(di-*n*-propylamino)cyclopropenium chloride[3,5] as the substrate. Compound **3-*n*Pr** was isolated as a white powder (25 mg, 41% yield) using 5% ethyl acetate in DCM as the eluent. R_F = 0.30 in 5% ethyl acetate/DCM. ^{1}H NMR (700 MHz, CD_3CN) δ 7.67 (d, *J* = 7.9 Hz, 2H), 7.58 (d, *J* = 7.8 Hz, 2H), 7.47 (t, *J* = 7.7 Hz, 2H), 7.40 (t, *J* = 7.6 Hz, 2H), 3.07 (t, *J* = 7.6 Hz, 8H), 1.48 (h, *J* = 7.9 Hz, 8H), 0.74 (t, *J* = 7.4 Hz, 12H). ^{13}C NMR (176 MHz, CD_3CN) δ 140.75, 134.25, 129.70, 129.67, 129.39, 125.31, 119.87, 112.50, 55.06, 22.38, 10.75. HRMS (ESI) *m/z* calcd for $C_{27}H_{36}N_3S^+$ (**3-*n*Pr**$^+$): 434.2624, found: 434.2615.

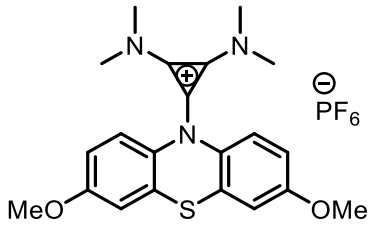

Synthesis of 4-Me: The general procedure was followed using 1-chloro-2,3-bis(dimethylamino)cyclopropenium chloride[3,5] as the substrate. Compound **4-Me** was isolated as a white powder (38 mg, 41%) using 8% ethyl acetate in DCM as the eluent. R_F = 0.21 in 8% ethyl acetate/DCM. ^{1}H NMR (400 MHz, CD_3CN) δ 7.51 (d, *J* = 8.8 Hz, 2H), 7.10 (d, *J* = 2.8 Hz, 2H), 6.95 (dd, *J* = 8.8, 2.8 Hz, 2H), 3.80 (s, 6H), 2.92 (s, 12H). ^{13}C NMR (126 MHz, CD_3CN) δ 159.97, 134.32, 133.52, 126.00, 120.36, 114.91, 114.16, 112.81, 56.60, 43.09. HRMS (ESI) *m/z* calcd for $C_{21}H_{24}N_3O_2S^+$ (**4-Me**$^+$): 382.1584, found: 382.1575.

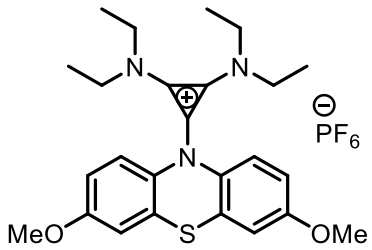

Synthesis of 4-Et: The general procedure was followed using 1-chloro-2,3-bis(diethylamino)cyclopropenium chloride[3,5] as the substrate. Compound **4-Et** was isolated as a white powder (40 mg, 39% yield) using 8% ethyl acetate in DCM as the eluent. R_F = 0.25 in 8% ethyl acetate/DCM. ^{1}H NMR (700 MHz, CD_3CN) δ 7.54 (d, *J* = 8.7 Hz, 2H), 7.12 (d, *J* = 2.8 Hz, 2H), 6.97 (dd, *J* = 8.7, 2.8 Hz, 2H), 3.81 (s, 6H), 3.14 (q, *J* = 7.2 Hz, 8H), 1.03 (t, *J* = 7.2 Hz, 12H). ^{13}C NMR (176 MHz, CD_3CN) δ 160.18, 135.71, 133.87, 126.43, 119.46, 114.94, 114.24, 113.95, 56.65, 48.02, 14.12. HRMS (ESI) *m/z* calcd for $C_{25}H_{32}N_3O_2S^+$ (**4-Et**$^+$): 438.2210, found: 438.2195.

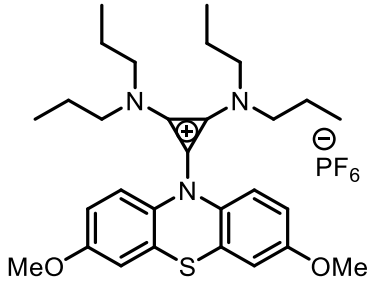

Synthesis of 4-^{n}Pr: The general procedure was followed using 1-chloro-2,3-bis(di-*n*-propylamino)cyclopropenium chloride[3,5] as the substrate. Compound **4-^{n}Pr** was isolated as a white powder (45 mg, 40% yield) using 8% ethyl acetate in DCM as the eluent. R_F = 0.27 in 8% ethyl acetate/DCM. ^{1}H NMR (500 MHz, CD_3CN) δ 7.55 (d, *J* = 8.7 Hz, 2H), 7.14 (d, *J* = 2.8 Hz, 2H), 6.97 (dd, *J* = 8.8, 2.8 Hz, 2H), 3.81 (s, 6H), 3.12-2.95 (m, 8H), 1.57-1.34 (m, 8H), 0.82-0.66 (m, 12H). ^{13}C NMR (126 MHz, CD_3CN) δ 160.16, 136.13, 133.98, 126.55, 119.72, 115.25, 114.39, 113.73, 56.68, 54.98, 22.31, 10.77. HRMS (ESI) *m/z* calcd for $C_{29}H_{40}N_3O_2S^+$ (**4-^{n}Pr$^+$**): 494.2836, found: 494.2838.

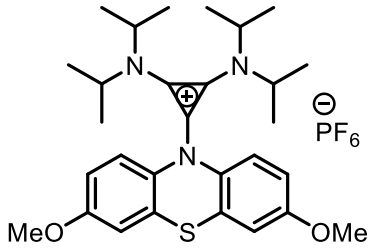

Synthesis of 4-^{i}Pr: The general procedure was followed using 1-chloro-2,3-bis(di-iso propylamino)cyclopropenium chloride[3,5] as the substrate. Compound **4-^{i}Pr** was isolated as a white powder (22 mg, 20% yield) using 8% ethyl acetate in DCM as the eluent. R_F = 0.24 in 8% ethyl acetate/DCM. ^{1}H NMR (400 MHz, CD_3CN) δ 6.87-6.81 (m, 4H), 6.72 (dd, *J* = 8.9, 2.9 Hz, 2H), 3.93 (hept, *J* = 6.9 Hz, 5H), 3.75 (s, 6H), 2.14 (s, 8H), 1.26 (d, *J* = 6.7 Hz, 26H). ^{13}C NMR (176 MHz, CD_3CN) δ 157.10, 132.34, 131.70, 123.89, 119.21, 112.81, 112.67, 104.99, 55.47, 52.76, 20.84. HRMS (ESI) *m/z* calcd for $C_{29}H_{40}N_3O_2S^+$ (**4-^{i}Pr$^+$**): 494.2836, found: 494.2832.

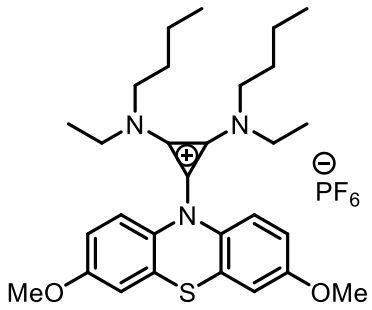

Synthesis of 4-EtBu: The general procedure was followed using 1-chloro-2,3-bis(ethylbutylamino)cyclopropenium chloride[3,5] as the substrate. Compound **4-EtBu** was isolated as a light-yellow viscous oil (50 mg, 45% yield) using 8% ethyl acetate in DCM as the eluent. R_F = 0.25 in 8% ethyl acetate/DCM. ^{1}H NMR (401 MHz, CD_3CN) δ 7.54 (d, *J* = 8.8 Hz, 2H), 7.13 (d, *J* = 2.8 Hz, 2H), 6.97 (dd, *J* = 8.7, 2.8 Hz, 2H), 3.81 (s, 6H), 3.16 (q, *J* = 7.2 Hz, 4H), 3.06 (t, *J* = 7.9 Hz, 4H), 1.44-1.29 (m, 4H), 1.15-0.98 (m, 10H), 0.84 (t, J = 7.3 Hz, 6H). ^{13}C NMR (176 MHz, CD_3CN) δ 160.16, 135.95, 133.93, 126.47, 119.60, 115.11, 114.29, 113.91, 56.66, 52.94, 48.53, 31.26, 20.19, 14.04, 13.98. HRMS (ESI) *m/z* calcd for $C_{29}H_{40}N_3O_2S^+$ (**4-EtBu**$^+$): 494.2836, found: 494.2829.

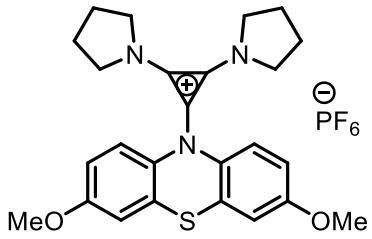

Synthesis of 4-Py: The general procedure was followed using 1-chloro-2,3-bis(pyrrolidino)cyclopropenium chloride[3,5] as the substrate. Compound **4-Py** was isolated as a white powder (52 mg, 52% yield) using 8% ethyl acetate in DCM as the eluent. R_F = 0.22 in 8% ethyl acetate/DCM. ^{1}H NMR (700 MHz, CD_3CN) δ 7.47 (d, *J* = 8.7 Hz, 2H), 7.05 (d, *J* = 2.8 Hz, 2H), 6.95 (dd, *J* = 8.8, 2.8 Hz, 2H), 3.81 (s, 6H), 3.53-3.25 (m, 8H), 1.93-1.86 (m, 8H). ^{13}C NMR (176 MHz, CD_3CN) δ 159.70, 132.95, 132.39, 124.70, 116.71, 114.76, 113.82, 110.81, 56.56, 52.58, 26.35. HRMS (ESI) *m/z* calcd for $C_{19}H_{22}N_3O^+$ (**4-Py**$^+$): 434.1897, found: 434.1889.

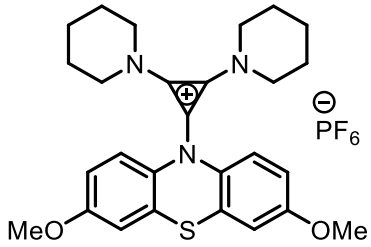

Synthesis of 4-Pip: The general procedure was followed using 1-chloro-2,3-bis(piperdino)cyclopropenium chloride[3,5] as the substrate. Compound **4-Pip** was isolated as a white powder (58 mg, 55% yield) using 8% ethyl acetate in DCM as the eluent. R_F = 0.24 in 8% ethyl acetate/DCM. ^{1}H NMR (500 MHz, CD_3CN) δ 7.47 (d, *J* = 8.7 Hz, 2H), 7.10 (d, *J* = 2.8 Hz, 2H), 6.96 (dd, *J* = 8.8, 2.8 Hz, 2H), 3.80 (s, 6H), 3.29-3.15 (m, 8H), 1.67-1.49 (multiple peaks, 12H). ^{13}C NMR (126 MHz, CD_3CN) δ 160.00, 134.53, 133.60, 125.68, 119.00, 114.81, 114.20, 112.89, 56.63, 52.68, 26.05, 23.60. HRMS (ESI) *m/z* calcd for $C_{27}H_{32}N_3O_2S^+$ (**4-Pip**$^+$): 462.2210, found: 462.2200.

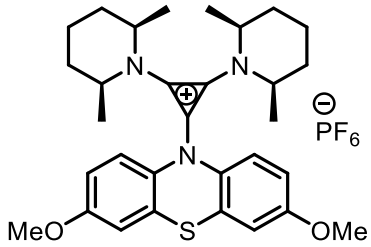

Synthesis of 4-DMPP: The general procedure was followed using 1-chloro-2,3-bis(cis-dimethylpiperdino)cyclopropenium chloride[3,5] as the substrate (2.4 mmol). Compound **4-DMPP** was isolated as a white powder (811 mg, 51% yield) using 8% ethyl acetate in DCM as the eluent. R_F = 0.25 in 8% ethyl acetate/DCM. ^{1}H NMR (700 MHz, CD_3CN) δ 7.54 (d, *J* = 8.7 Hz, 2H), 7.14 (d, *J* = 2.3 Hz, 2H), 6.97 (dd, *J* = 8.8, 2.8 Hz, 2H), 3.81 (s, 6H), 3.60-3.38 (m, 4H), 1.76-1.68 (m, 2H), 1.68-1.60 (m, 4H), 1.53-1.41 (m, 6H), 1.13 (d, J = 7.0 Hz, 12H). ^{13}C NMR (176 MHz, CD_3CN) δ 160.26, 136.79, 134.32, 127.29, 120.11, 115.03, 114.93, 114.34, 56.69, 54.78, 29.99, 21.53, 13.02. HRMS (ESI) *m/z* calcd for $C_{31}H_{40}N_3O_2S^+$ (**4-DMPP**$^+$): 518.2836, found: 518.2826.

II. NMR spectra

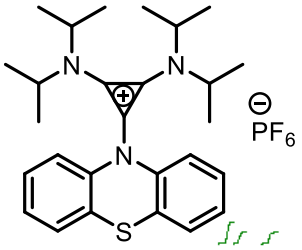

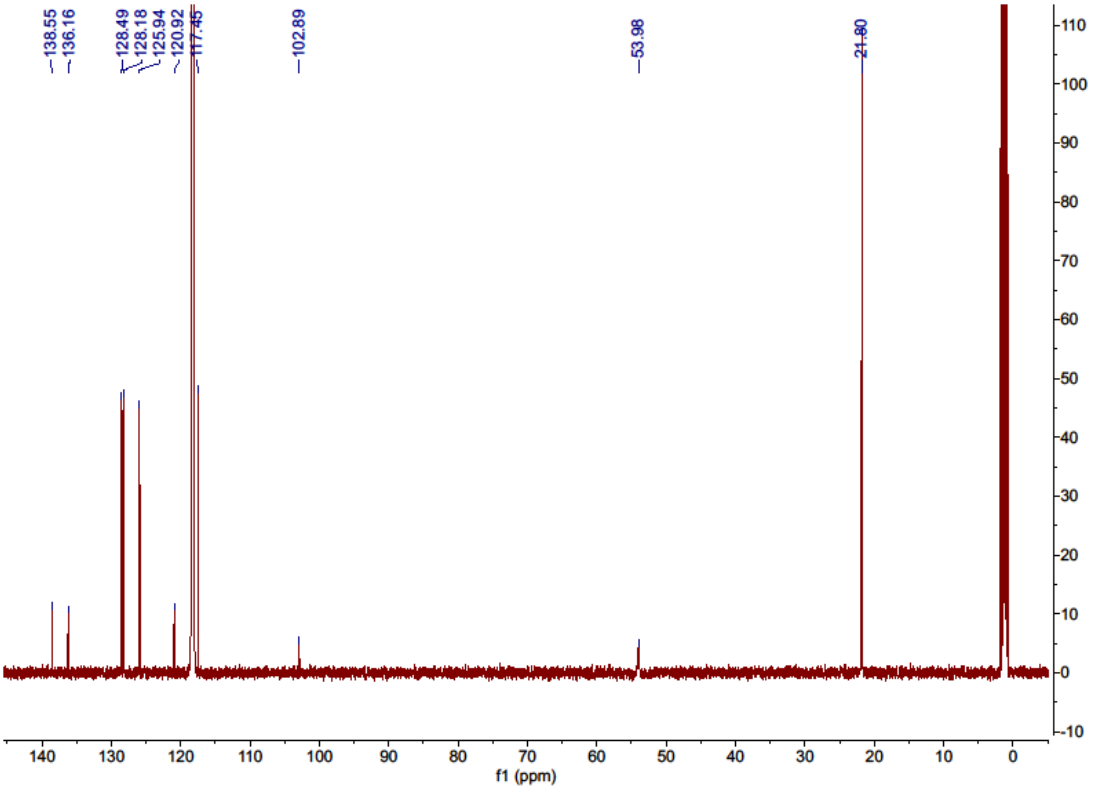

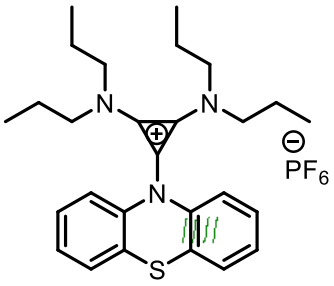
N
N
N
S
PF6

1.00
0.95
1.03
1.02
4.26
4.18
6.27
f1 (ppm)

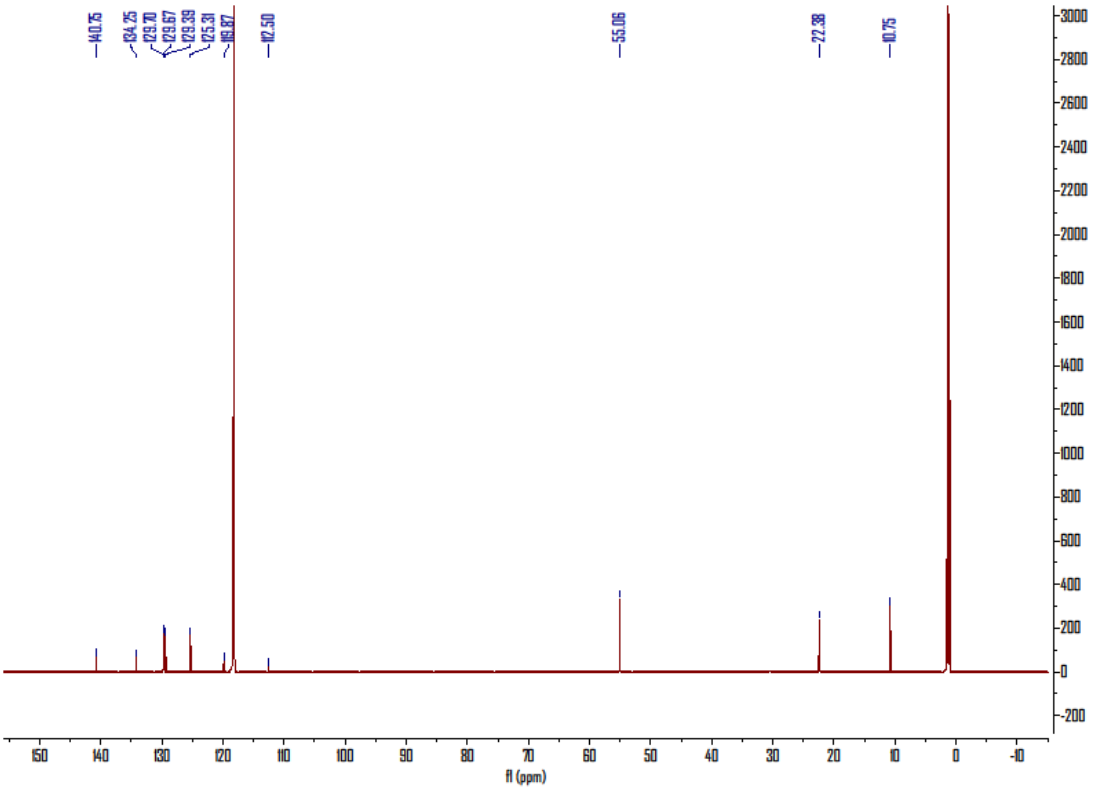
140.75
134.25
129.70
129.67
129.39
125.31
116.87
112.50
55.06
22.38
10.75
f1 (ppm)

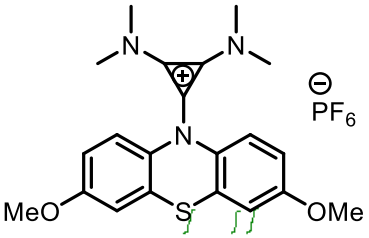
N
N
N
S
MeO
OMe
PF6

2.00
1.87
2.04
6.49
12.49
f1 (ppm)

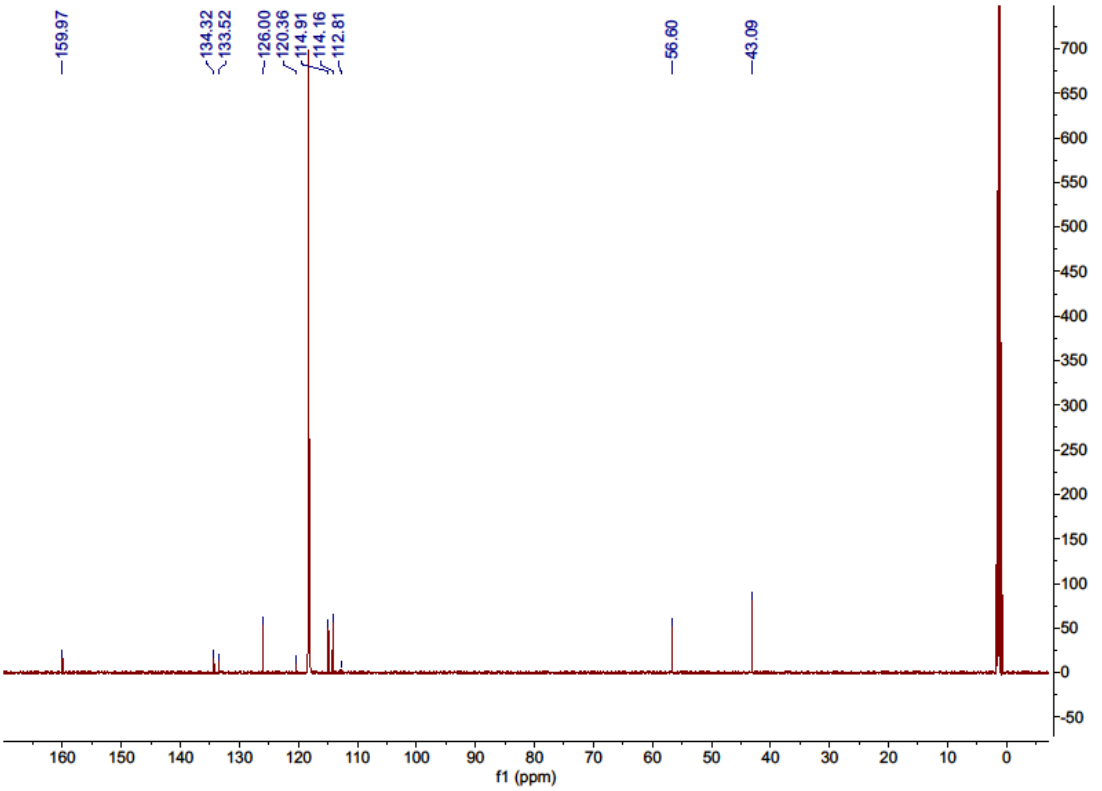
159.97
134.32
133.52
126.00
120.36
114.91
114.16
112.81
56.60
43.09
f1 (ppm)

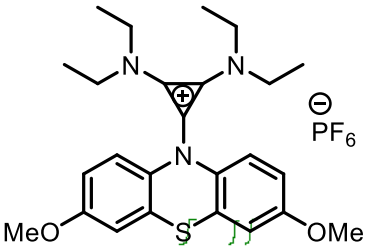
N
N
N
S
MeO
OMe
PF6

2.00
1.86
2.01
6.33
8.02
12.23
f1 (ppm)

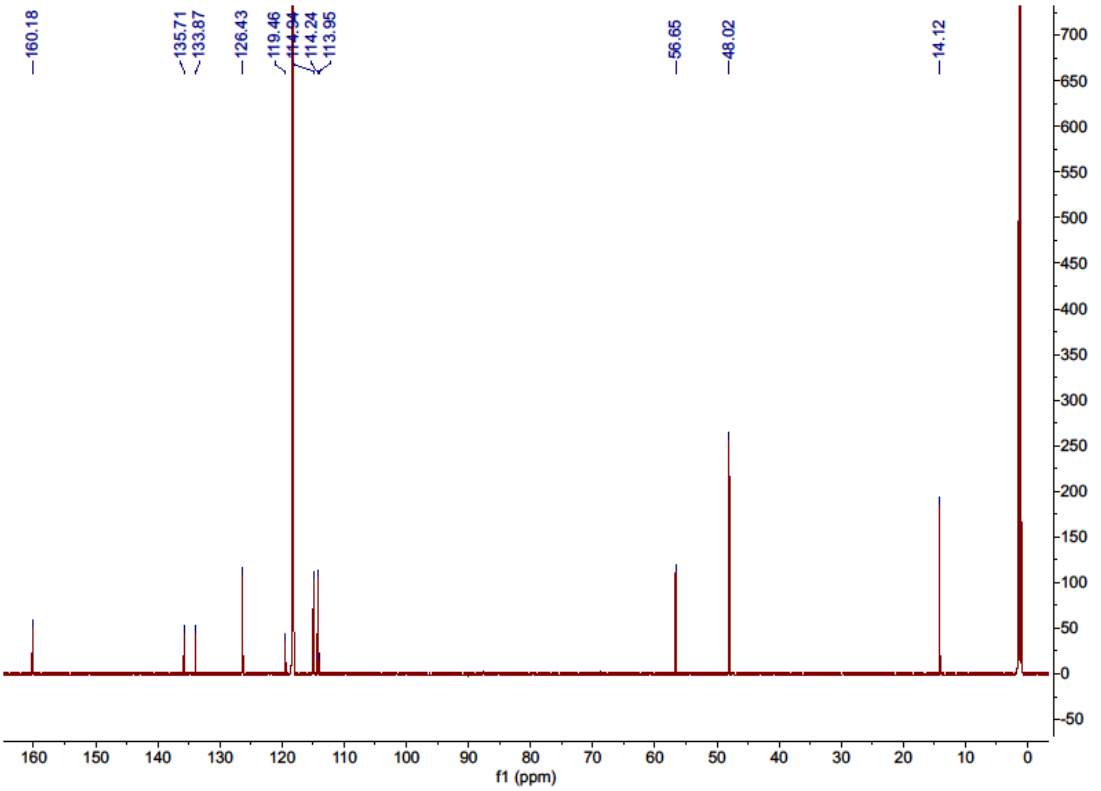
160.18
135.71
133.87
126.43
119.46
114.24
113.95
56.65
48.02
14.12
f1 (ppm)

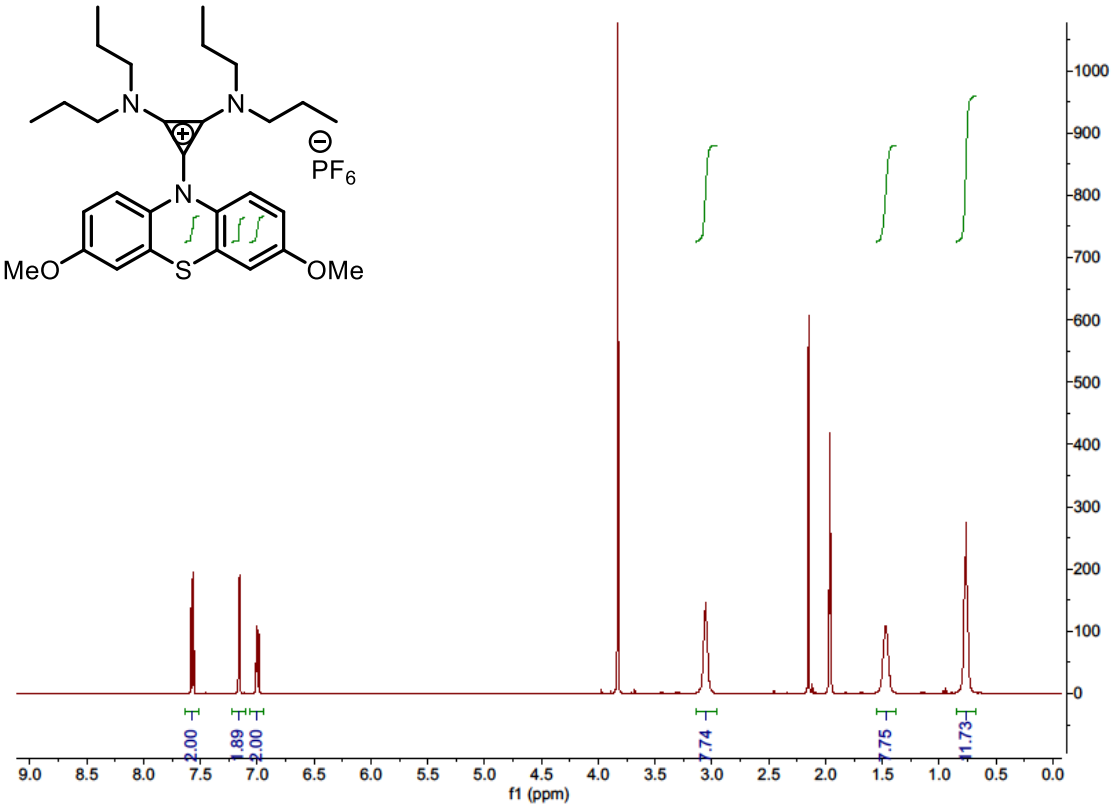
N
N
N
⊖
PF6
MeO
S
OMe
2.00
1.89
2.00
7.74
7.75
11.73
f1 (ppm)

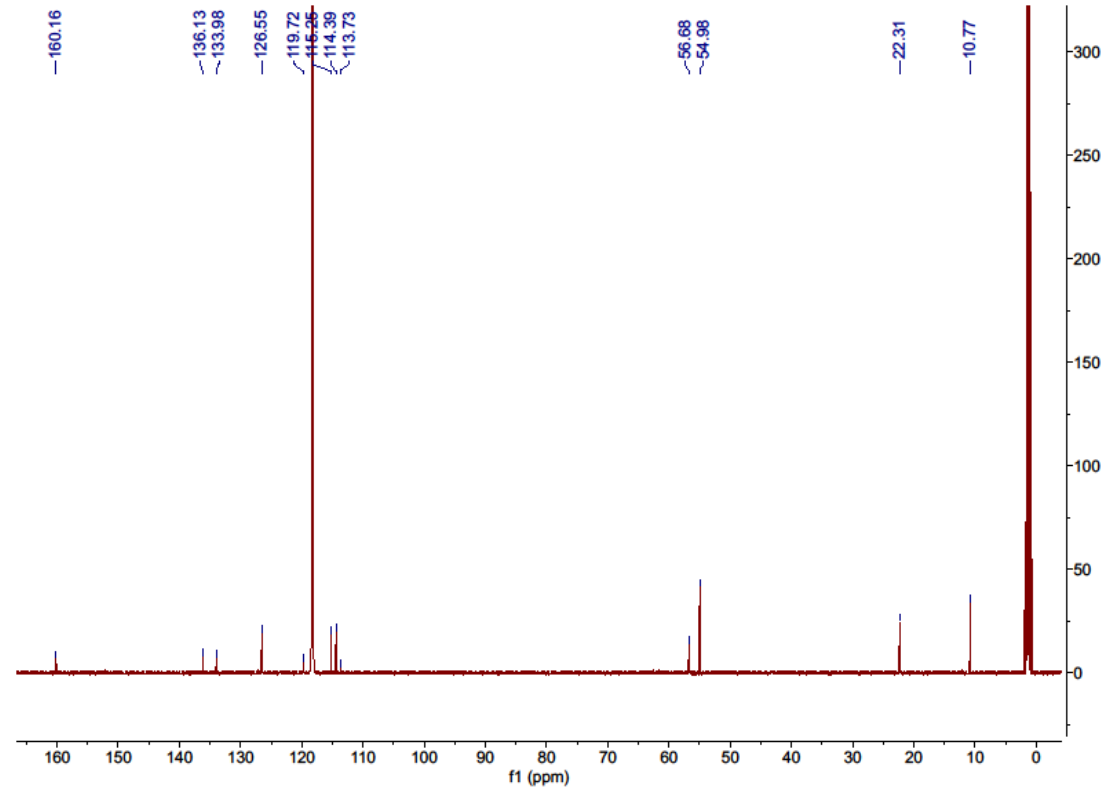
160.16
136.13
133.98
126.55
119.72
115.25
114.39
113.73
56.68
54.98
22.31
10.77
f1 (ppm)

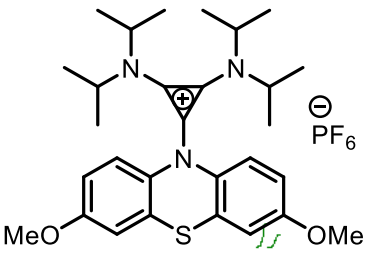
N
N
N
S
MeO
OMe
PF6

4.00
2.06
4.61
6.49
7.73
26.01
f1 (ppm)

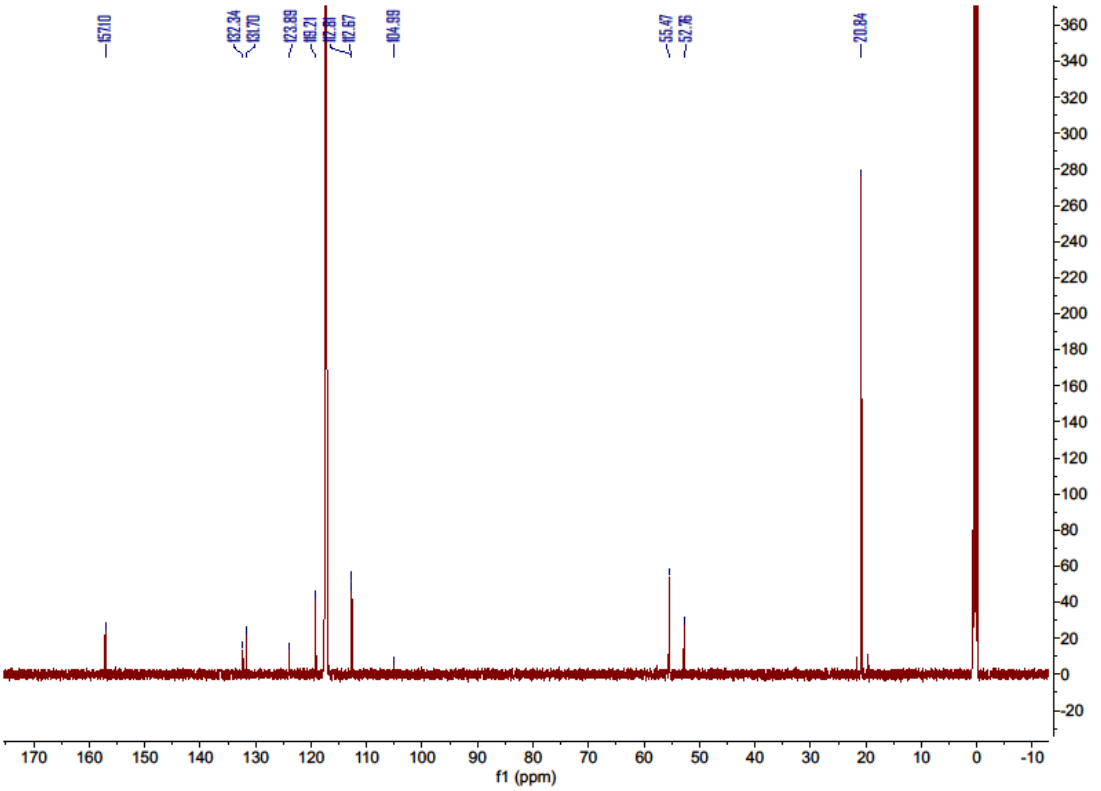
157.10
132.34
131.70
123.88
119.21
112.86
112.67
104.99
55.47
52.76
20.84
f1 (ppm)

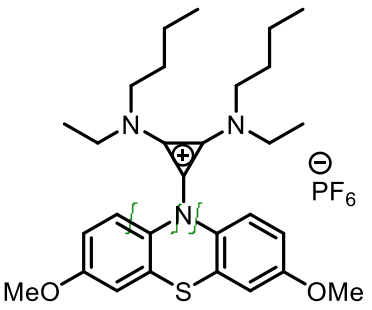
N
N
N
S
MeO
OMe
PF6

2.00
1.87
1.99
6.28
3.78
3.86
3.72
9.80
6.17
f1 (ppm)

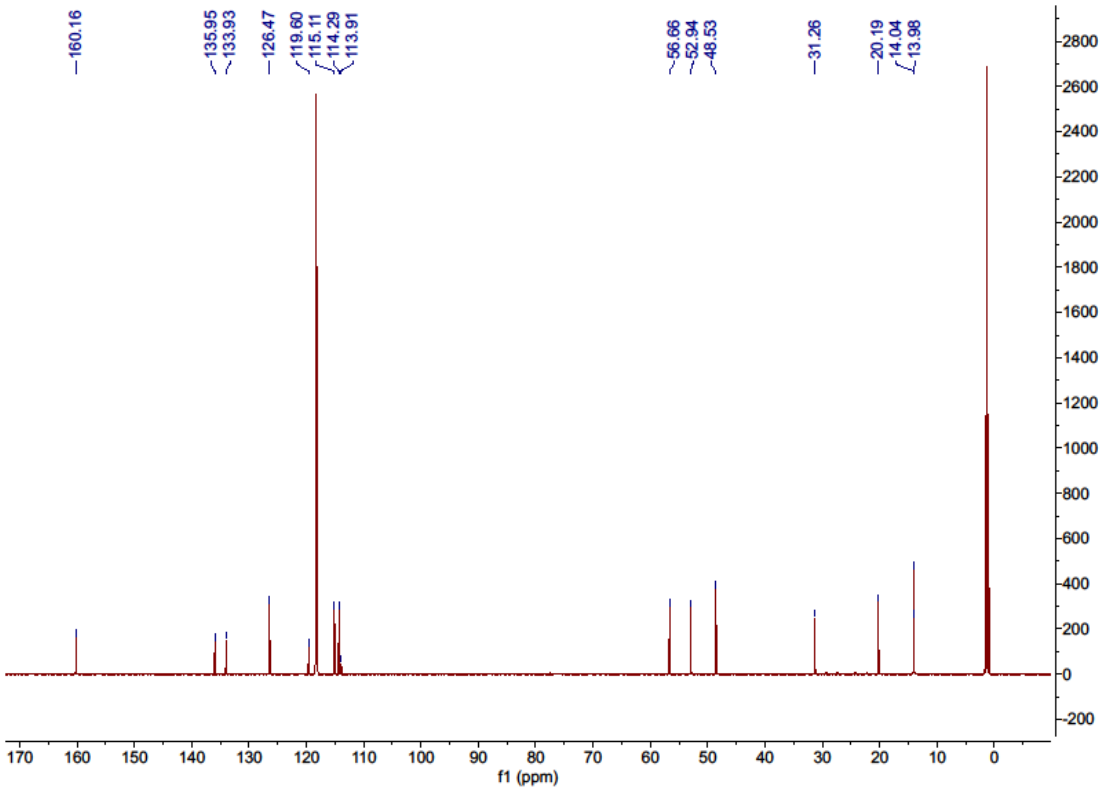
160.16
135.95
133.93
126.47
119.60
115.11
114.29
113.91
56.66
52.94
48.53
31.26
20.19
14.04
13.98
f1 (ppm)

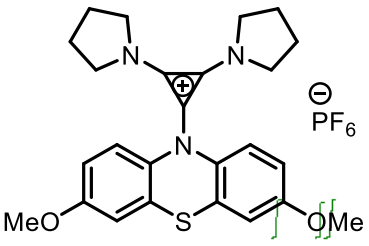
N
N
PF6
N
MeO
S
OMe

2.00
1.86
2.02
6.35
7.70
7.51
f1 (ppm)

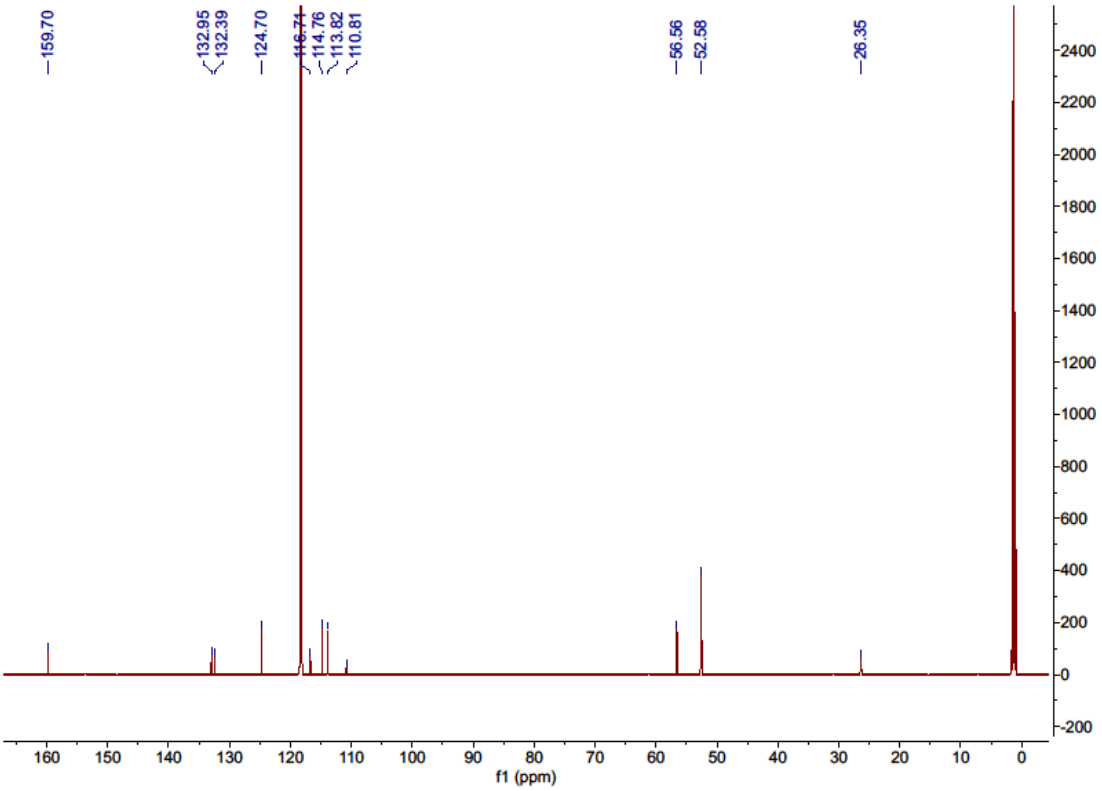
159.70
132.95
132.39
124.70
116.71
114.76
113.82
110.81
56.56
52.58
26.35
f1 (ppm)

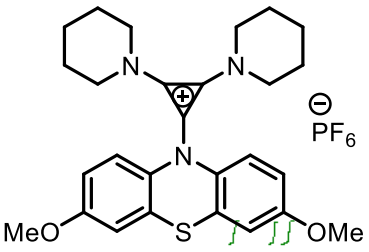
N
N
N
S
MeO
OMe
PF6

2.00
1.88
2.01
6.26
8.36
12.60
f1 (ppm)

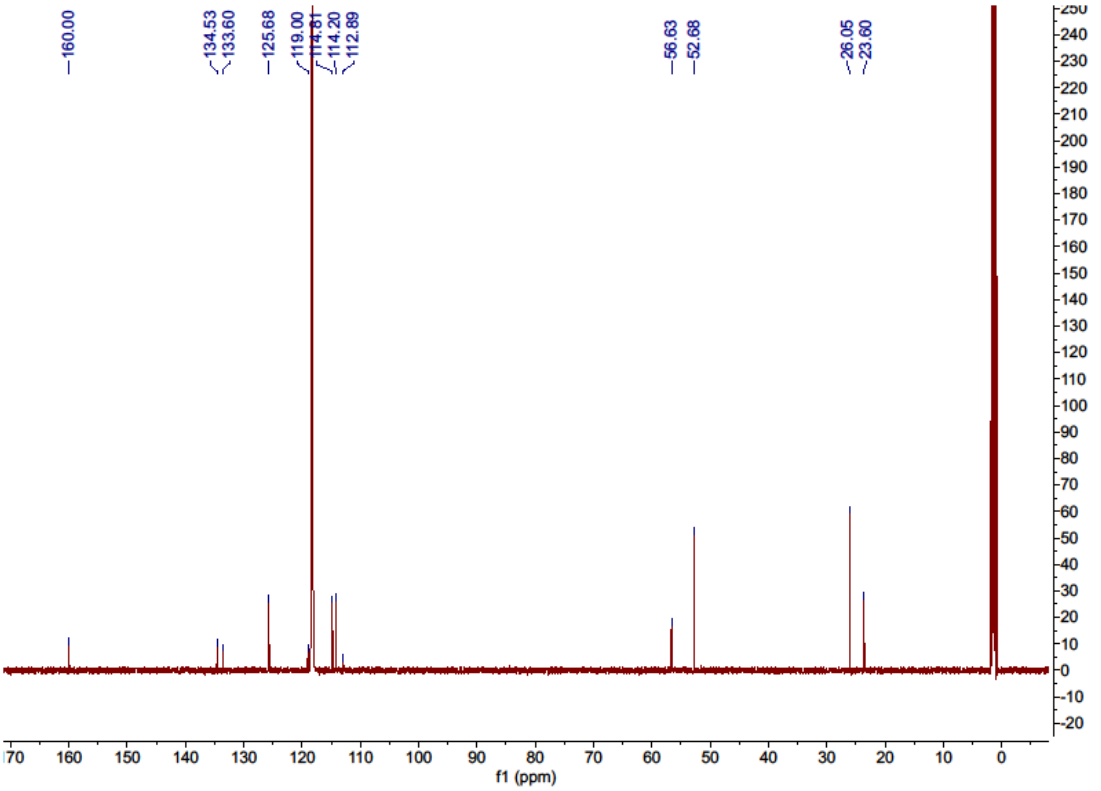
160.00
134.53
133.60
125.68
119.00
114.81
114.20
112.89
56.63
52.68
26.05
23.60
f1 (ppm)

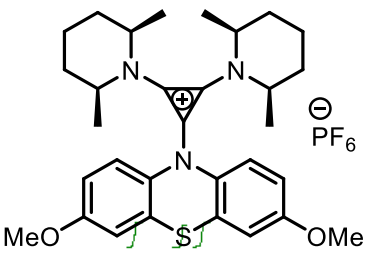
N
N
N
S
MeO
OMe
PF6

2.00
1.84
1.99
6.27
3.77
2.14
4.08
6.12
12.25
f1 (ppm)

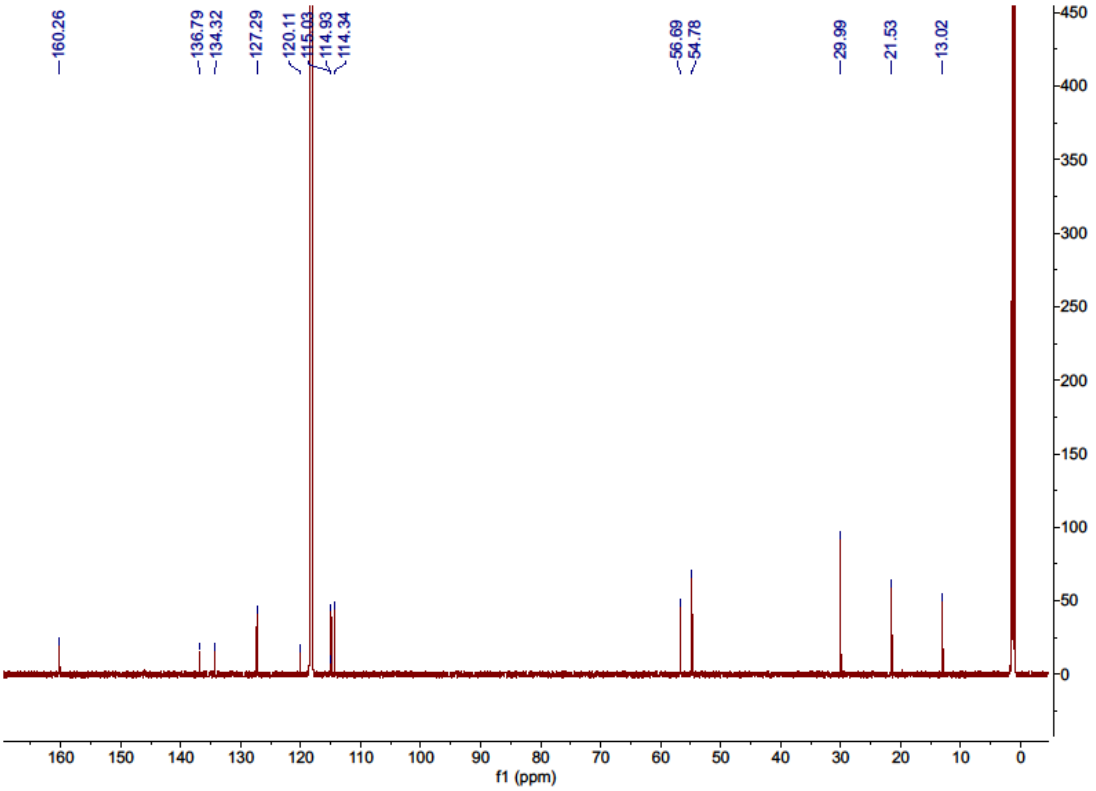
160.26
136.79
134.32
127.29
120.11
115.03
114.93
114.34
56.69
54.78
29.99
21.53
13.02
f1 (ppm)

III. X-ray Crystallographic Data for 4-DMPP

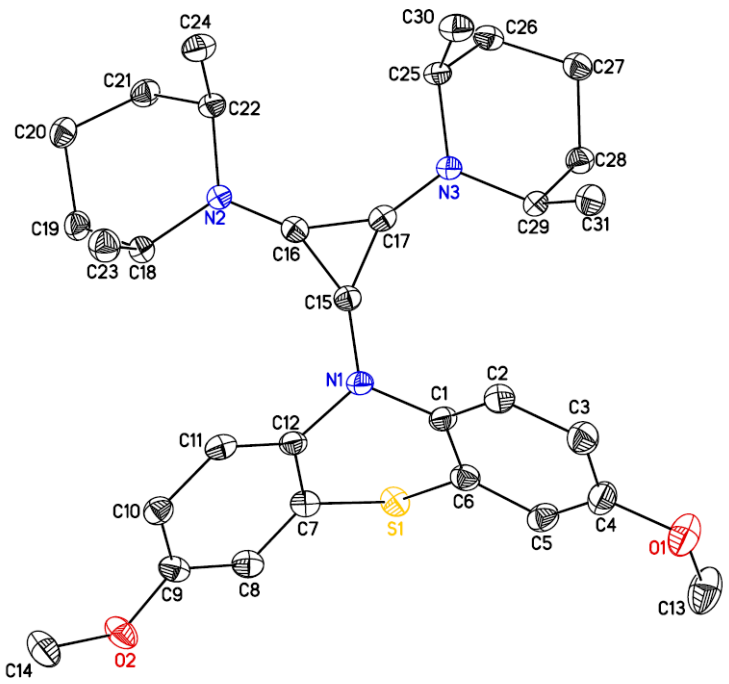

Figure S1. PLUTO representation of **4-DMPP**. The PF_6 anions are omitted for clarity.

Structure Determination.

Colorless blocks of **4-DMPP** were grown from an ethyl acetate/diethyl ether solution of the compound at -30 deg. C. A crystal of dimensions 0.18 x 0.11 x 0.08 mm was mounted on a Rigaku AFC10K Saturn 944+ CCD-based X-ray diffractometer equipped with a low temperature device and Micromax-007HF Cu-target micro-focus rotating anode (λ = 1.54187 A) operated at 1.2 kW power (40 kV, 30 mA). The X-ray intensities were measured at 85(1) K with the detector placed at a distance 42.00 mm from the crystal. A total of 2028 images were collected with an oscillation width of 1.0° in ω. The exposure times were 1 sec. for the low angle images, 5 sec. for high angle. Rigaku d*trek images were exported to CrysAlisPro for processing and corrected for absorption. The crystal was determined to be a two component, non-merohedral twin. The twin domains are related by a -179.97 deg. Rotation about the direct space 91 0 0) vector and a refined twin ratio of 0.515(1). Reflections from both components as well as overlaps were used as the basis of an HKLF% format reflection file for refinement. The integration of the data yielded a total of 84874 reflections to a maximum 2θ value of 139.37° of which 13148 were independent and 9701 were greater than 2σ(I). The final cell constants (Table 1) were based on the xyz centroids of 14463 reflections above 10σ(I). Analysis of the data showed negligible decay during data collection. The structure was solved and refined with the Bruker SHELXTL (version 2018/3) software package, using the space group P2(1)/c with Z = 4 for the formula $C_{35}H_{50}N_3O_3F_6PS$. All non-hydrogen atoms were refined anisotropically with the hydrogen atoms placed in idealized

positions. Full matrix least-squares refinement based on F^2 converged at R1 = 0.0524 and wR2 = 0.1391 [based on I > 2sigma(I)], R1 = 0.0670 and wR2 = 0.1440 for all data. Additional details are presented in Table 1 and are given as Supporting Information in a CIF file. Acknowledgement is made for funding from NSF grant CHE-0840456 for X-ray instrumentation.

Table S1. Crystal data and structure refinement for **4-DMPP**.

Empirical formula	$C_{35}H_{50}F_6N_3O_3PS$
Formula weight	737.81
Temperature	85(2) K
Wavelength	1.54184 A
Crystal system, space group	Monoclinic, P2(1)/c
Unit cell dimensions	a = 15.4786(5) Å alpha = 90°
	b = 27.7901(8) Å beta = 92.250(3)°
	c = 8.4187(2) Å gamma = 90°
Volume	3618.51(19) $Å^3$
Z, Calculated density	4, 1.354 Mg/m^3
Absorption coefficient	1.818 mm^{-1}
F(000)	1560
Crystal size	0.180 x 0.110 x 0.080 mm
Theta range for data collection	2.857 to 69.684°
Limiting indices	–17<=h<=18, –33<=k<=33, –10<=l<=10
Reflections collected / unique	84874 / 13148 [R(int) = 0.0951]
Completeness to theta = 67.684	100.0 %
Absorption correction	Semi-empirical from equivalents
Max. and min. transmission	1.00000 and 0.70179
Refinement method	Full-matrix least-squares on F^2
Data / restraints / parameters	13148 / 0 / 451
Goodness-of-fit on F^2	1.004
Final R indices [I>2sigma(I)]	R1 = 0.0524, wR2 = 0.1391
R indices (all data)	R1 = 0.0670, wR2 = 0.1440

Extinction coefficient	n/a
Largest diff. peak and hole	0.732 and –0.466 eÅ^{-3}

IV. Electrochemistry Experimental Procedures

General methods and materials. Acetonitrile (anhydrous, 99.8%) was obtained from Sigma Aldrich and used as received. Tetrabutylammonium hexafluorophosphate ($TBAPF_6$; electrochemical grade) was obtained from Sigma Aldrich and dried under high vacuum for 48 h at 80 °C before being transferred to a N_2-filled glovebox. A 0.50 M stock solution of $TBAPF_6$ in acetonitrile was prepared in a N_2-filled glovebox and dried over 3Å molecular sieves for at least two days prior to use. Celgard-4560 membrane was provided by Celgard company and Daramic-175 membrane was provided by Daramic company. Both were used as received. The solubility of **4-DMPP**$^{++}$ in 0.5 M $TBAPF_6$/MeCN was determined using a previously reported method.[6]

Cyclic voltammetry. Cyclic voltammetry (CV) was performed in a N_2-filled glovebox with a Biologic VSP multichannel potentiostat/galvanostat using a three-electrode electrochemical cell, consisting of a glassy carbon disk working electrode (0.071 cm^2, BASi), a Ag/Ag$^+$ reference electrode (BASi) with 0.01 M $AgBF_4$ (Sigma) and 0.5 M $TBAPF_6$ in acetonitrile, and a platinum wire counter electrode. All experiments were conducted in a 0.50 M $TBAPF_6$/acetonitrile electrolyte stock solution.

H-cell cycling. Bulk charge/discharge measurements were carried out in a N_2-filled glovebox with a BioLogic VSP galvanostat in a custom glass H-cell with an ultrafine fritted glass separator (P5, Adams and Chittenden). The working and counter electrodes were reticulated vitreous carbon (100 ppi, ~70 cm^2 surface area, Duocel). A Ag/Ag$^+$ reference electrode was used on the working side of the H-cell. The electrolyte contained 2.5 mM active species and 0.50 M $TBAPF_6$ in acetonitrile. Both chambers of the H-cell were loaded with 5 mL of electrolyte solution and were stirred continuously during cycling at a current of 5 mA. Voltage cutoffs of +0.5 V higher than $E_{1/2}$ as the upper limit and -0.5 V lower than $E_{1/2}$ as the lower limit were employed.

Flow cell cycling. Cycling under flow conditions was performed with a zero-gap flow cell

comprised of graphite charge collecting plates containing an interdigitated flow field in combination with two layers of non-woven carbon felt electrodes (Sigracet 29AA) on each side.[7] PTFE gaskets were used to achieve ~20% compression of the felt. One Celgard 4560 or Daramic 175 membrane separated the two half cells, and the exposed area of the membrane in the gasket window was used as the active area (2.55 cm^2). After assembly, both sides are filled with a 50 mM solution of the catholyte and a 50 mM solution of the anolyte in 0.5 M $TBAPF_6$ (Figure 4a) or 0.3 M catholyte and 0.6 M anolyte in 0.5 M $TBAPF_6$ (Figure 5a). The cell was pretreated by continuously flowing the solutions above at 10 mL/min for 1 h without any charging process using a peristaltic pump (Cole-Parmer) with Solve-Flex and PFA tubing. After this step, using the same flow rate, galvanostatic charge/discharge cycling was performed using a BioLogic VSP galvanostat employing a certain charging/discharging current. Electrochemical impedance spectroscopy (EIS) was performed before and after cycling from 500 kHz to 1 Hz at OCV using a 10-mV sine perturbation.

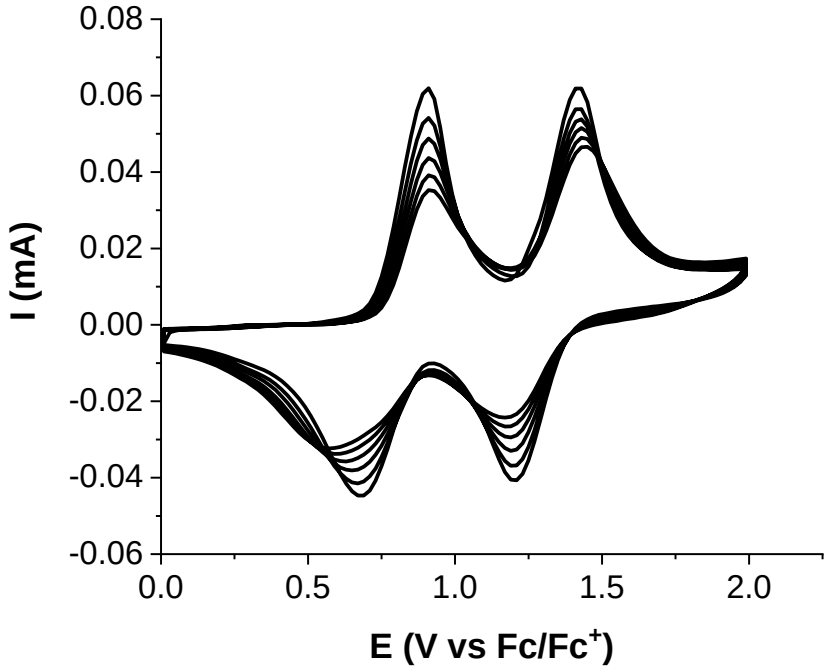

Figure S2. CV of **3-^{n}Pr** (5 cycles) CVs conducted with a 5 mM solution in 0.5 M NBu_4PF_6/MeCN at 100 mV/s scan rate.

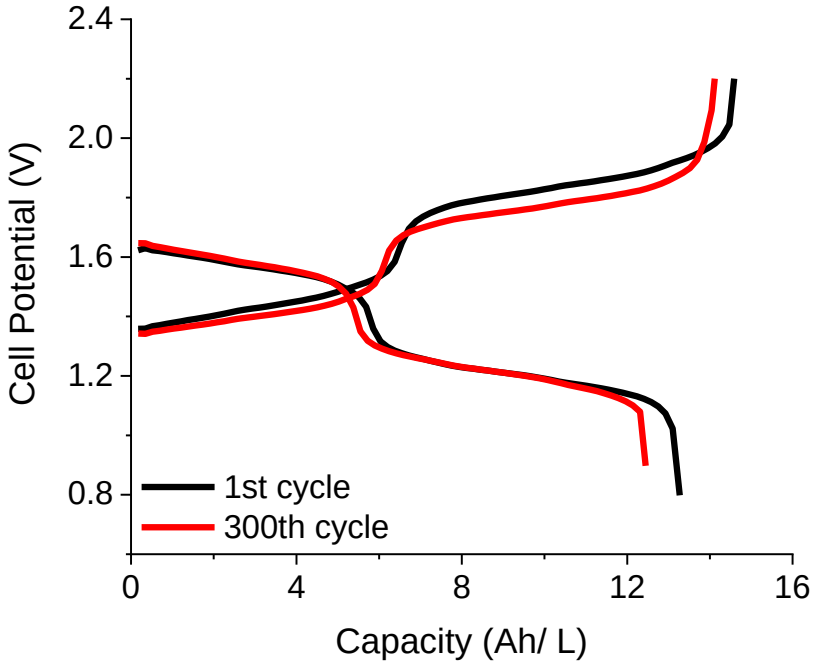

Figure S3. Charge and Discharge curves of the high concentration cycling using **4-DMPP** and **5**.

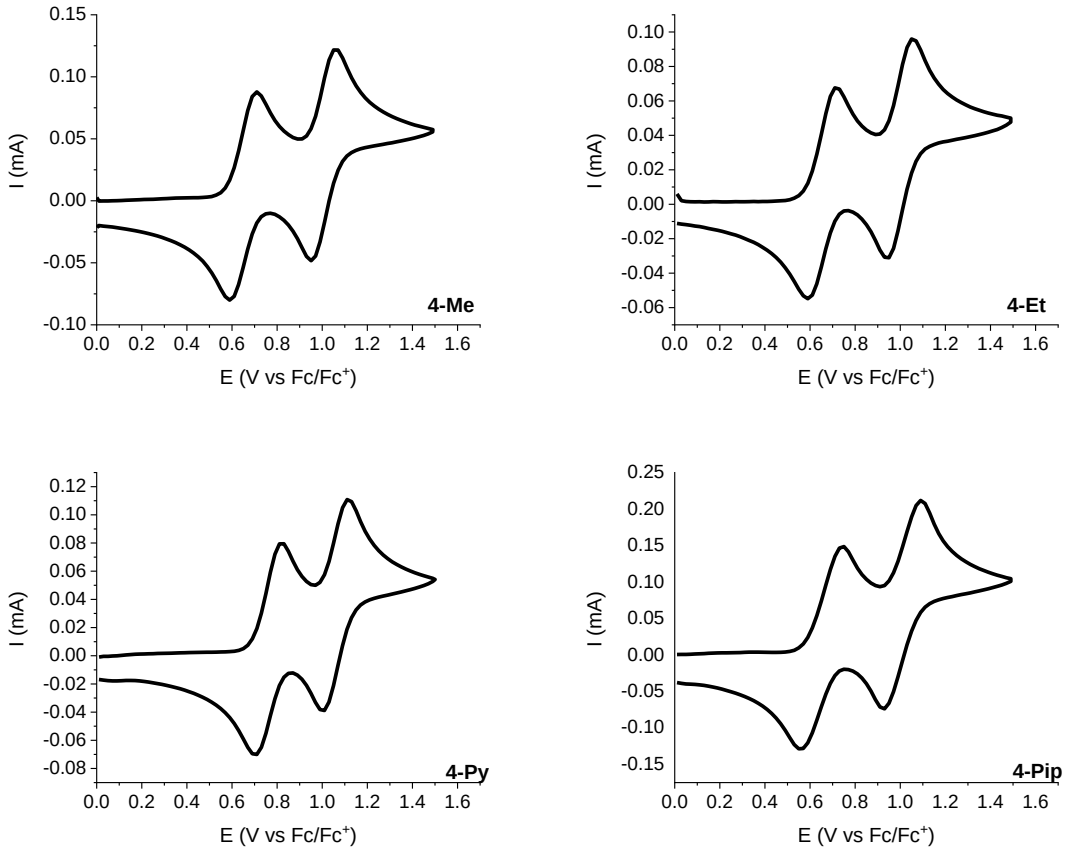

Figure S4. CV for series **4** compounds not showing in the main article (5 mM active materials in 0.5 M $TBAPF_6$)

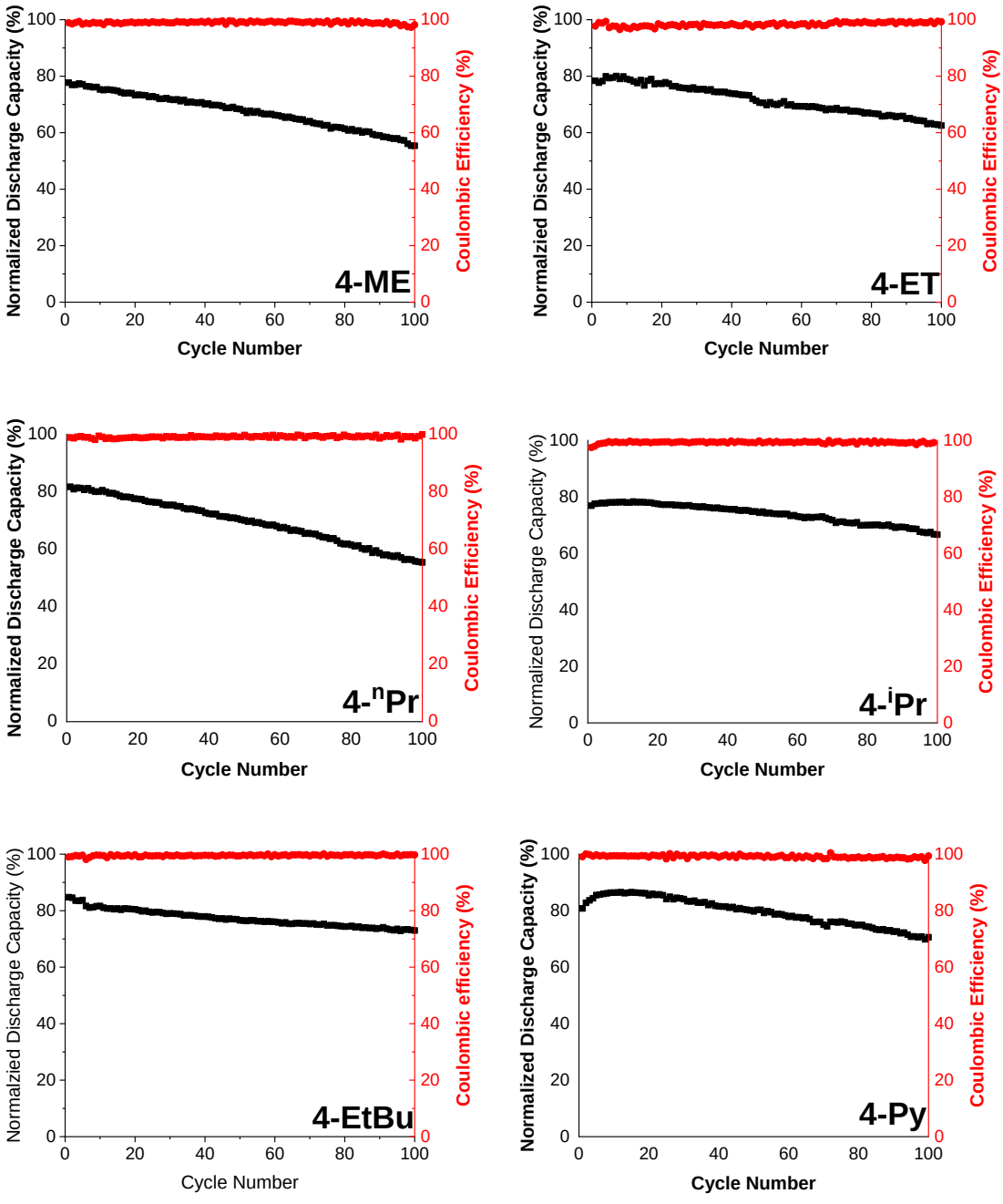

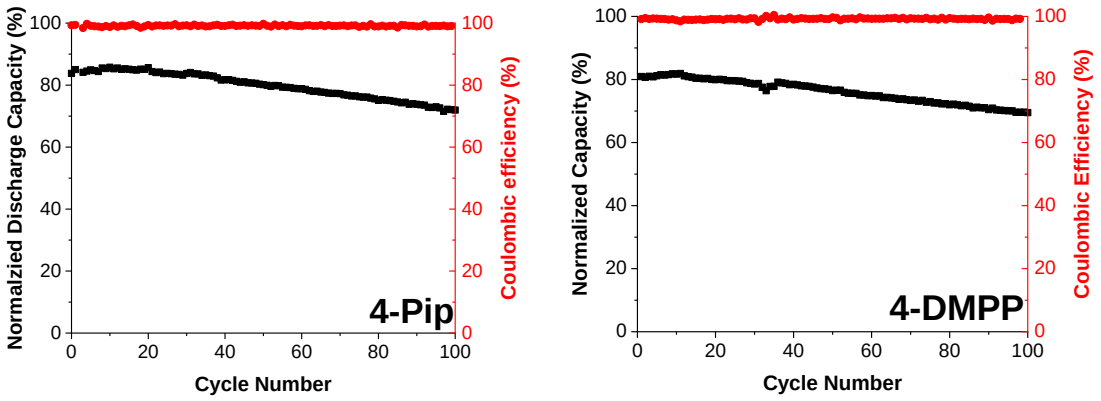

Figure S5. Bulk electrolysis data for series **4** compounds (2.5 mM active materials in 0.5 M $TBAPF_6$)

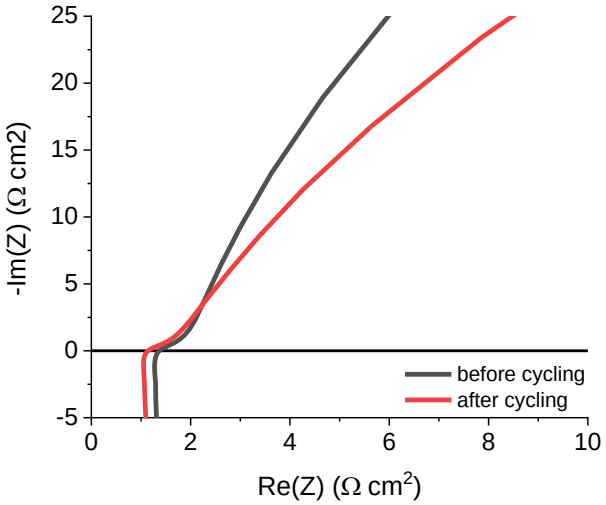

Figure S6. Electrochemical impedance spectroscopy (EIS) on cells for before and after for Figure 5

Determination of the Diffusion Coefficient and Electron Transfer Rate Constant of 4-DMPP.

The diffusion coefficient was determined by varying the scan rate of CV measurements between 20 and 700 mV/s (Figure S3, left). Plotting the cathodic and anodic peak height currents versus the square root of the scan rate showed a linear relationship, indicating a transport-limited redox process (Figure S3, right). The slope of this linear relation was used

in the Randles-Sevcik equation (eq 1) to determine the diffusion coefficient.[8]

$$i_p = 0.4463\, nFAC\sqrt{\frac{nFvD}{RT}} \qquad (1)$$

The terms of the equation: i_p is the peak current in amps, n is the number of electrons transferred, F is Faraday's constant, A is the area of the electrode in cm^2, C *is* the concentration of redox active species in mol cm^{-3}, D is the diffusion coefficient in $cm^2\ s^{-1}$, v is the scan rate in $V\ s^{-1}$, R is the gas constant in $JK^{-1}mol^{-1}$, and T is the temperature in K.

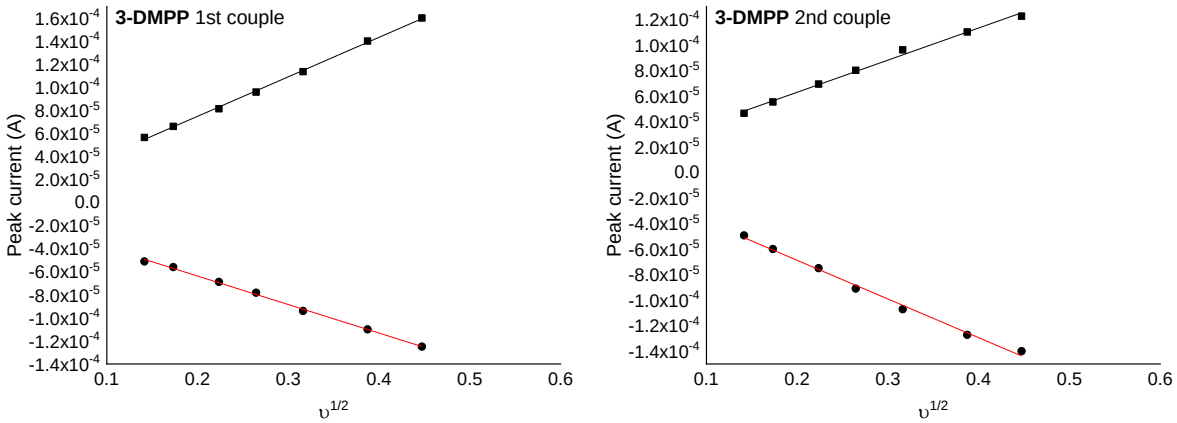

Figure S7. Peak current (A) vs square root of the scan rate ($v^{½}$) and linear fits used to determine diffusion coefficients.

The heterogeneous electron transfer rate constant was determined following the Nicholson method.[9] The peak separations between the cathodic and anodic peaks at various scan rates were fit to a working curve. Plotting the resulting values of Nicholson dimensionless number Ψ versus the inverse square root of the scan rate (Figure S4) gave a relationship from which the slope was used to determine k_0 according to eq 2,

$$\psi = \frac{\gamma k_0}{\sqrt{\pi a D_0}} \qquad (2)$$

where k_0 is the standard rate constant in $cm\ s^{-1}$; Ψ is the Nicholson dimensionless number, which is a function of the peak potential separation ($\boldsymbol{\Delta E_p}$) from CV curve. D_0 is the diffusion coefficient in $cm^2\ s^{-1}$. α is the charge transfer coefficient, dimensionless. $\gamma = \sqrt{\frac{RT}{nF}}$, where n is the number of electrons transferred in the redox reaction, F is Faraday's constant (96485 C mol^{-1}), R is the ideal gas constant (8.314 J mol K^{-1}), T is the absolute temperature in K.

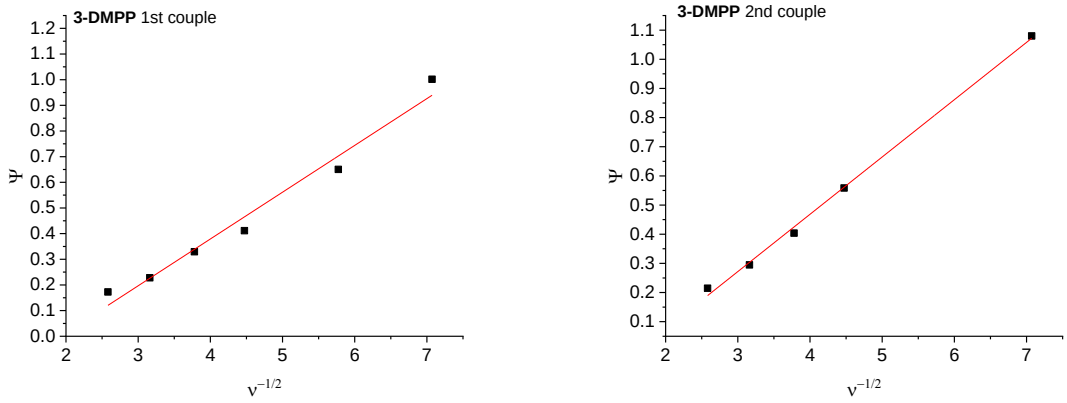

Figure S8. Plots of the Nicholson dimensionless number (Ψ) versus inverse of the scan rate ($\nu^{1/2}$). A linear fit was used to determine heterogeneous electron transfer rates.

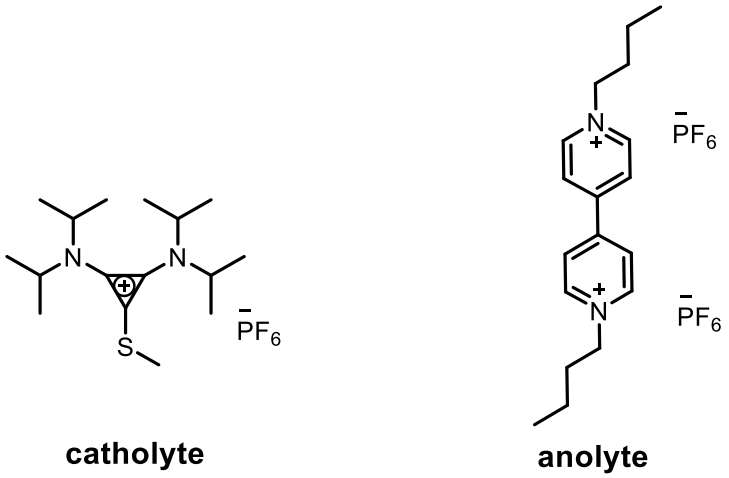

catholyte **anolyte**

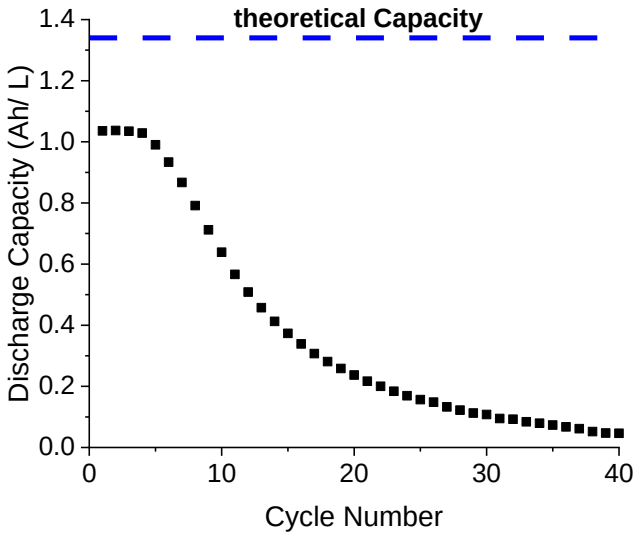

95% capacity loss at 40 cycles

Figure S9. Flow cell cycling of 50 mM thio-CP as catholyte and 50 mM viologen derivative as anolyte (1:1 mixture solution in both reservoirs, Daramic 175 membrane, 10 mA/ cm^2).

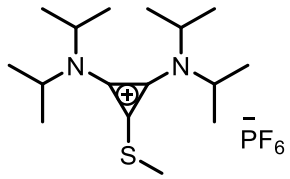

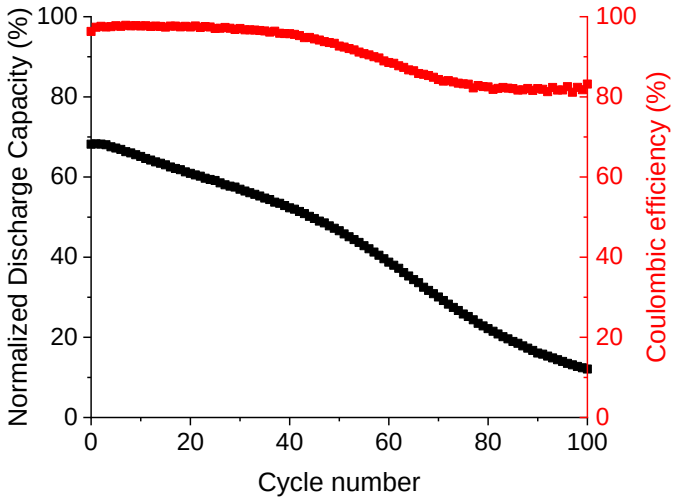

83% capacity loss at 100 cycles

Figure S10. H-Cell bulk electrolysis data for thio-CP (5 mM active material in 0.5 M $TBAPF_6$; with only voltage cutoff)

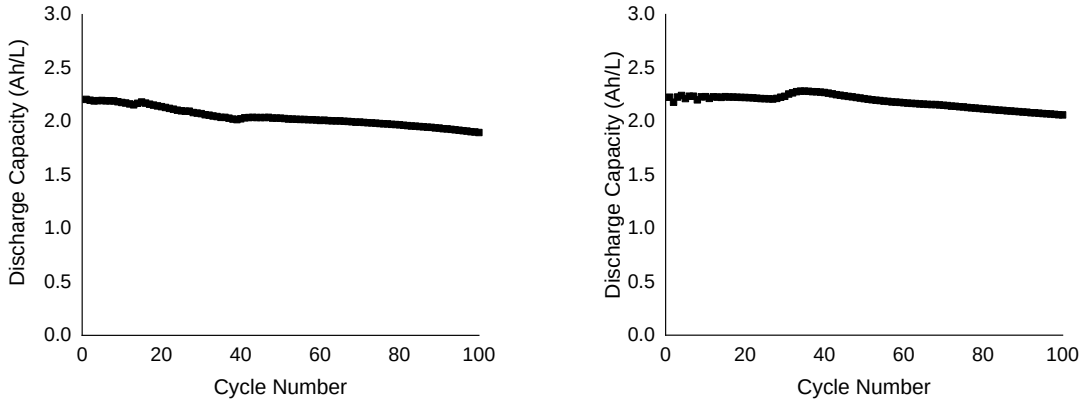

Figure S11. Flow cell cycling of 50 mM **4-DMPP** or **4-EtBu** as catholyte and 50 mM **5** as anolyte (two different trials of the **4-DMPP** cycling).

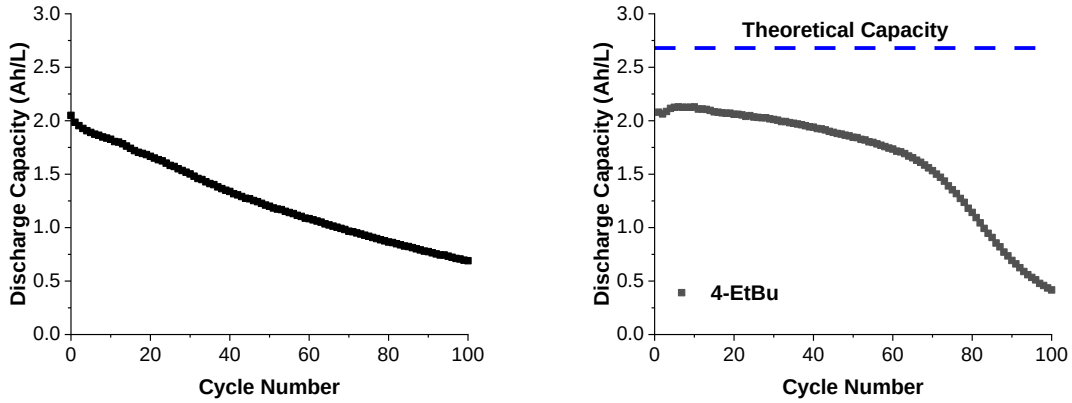

Figure S12. Flow cell cycling of 50 mM **4-EtBu** as catholyte and 50 mM **5** as anolyte **(left: wrapping the entire apparatus with Al foil; right: with light exposure)**

This experiment was setup to investigate the impact of light on the decomposition of **4-EtBu** during flow cell cycling Al foil was used limit light exposure to the flow cell during cycling.

V. Representative Reported Non-aqueous Catholytes

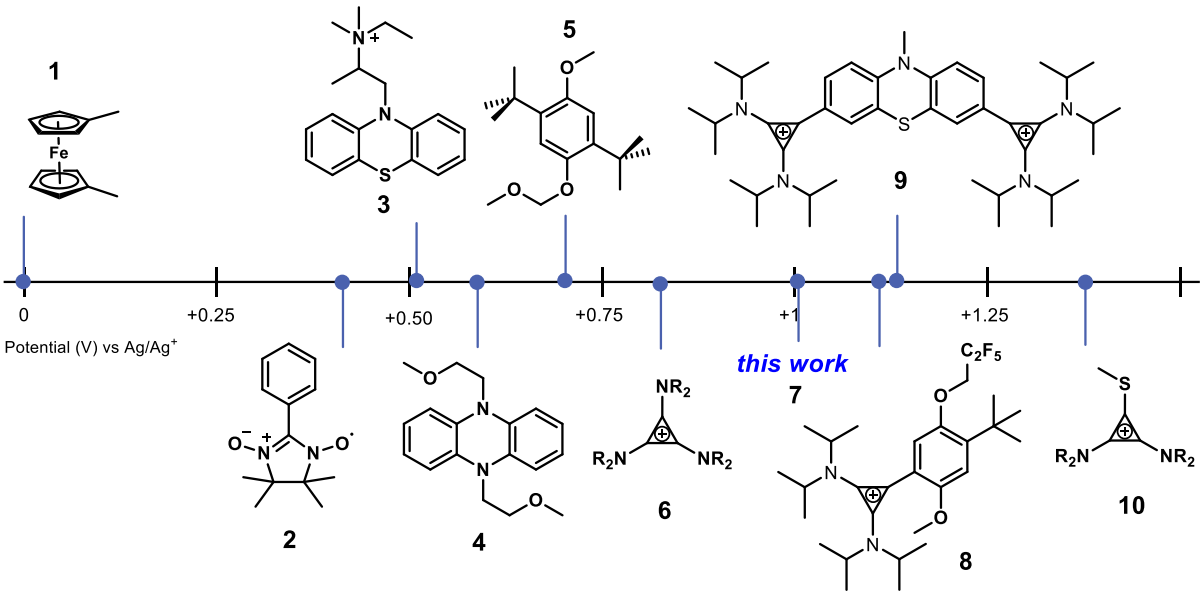

Table S2. Representative reported organic catholytes and their high concentration flow batteries

Compound	Redox Potential	Cyclability (electron conc.)	Energy Density (discharge)
1[10]	-0.045 V vs Ag/Ag^+	87% capacity for 100 cycles (0.5 M)	7.2 W h/L
2[11]	0.46 V vs Ag/Ag^+	~ 50% capacity for 15 cycles (0.5 M)	5 W h/L
3[12]	0.55 V vs Fc/Fc^+	84% capacity for 35 cycles (0.75M)	14.3 Wh /L
4[13]	1^{st}: -0.15 V; 2^{nd} : 0.6 V vs Ag/Ag^+	~83% capacity for 25 cycles (0.8 M)	12.9 Wh /L
5[14]	0.69 V vs Ag/Ag^+	~80% capacity for 50 cycles (0.5 M)	6-8 Wh /L
6[15]	0.82 V vs Fc/Fc^+	95% capacity for 200 cycles (0.05 M)	0.85 Wh /L
7 (this work)	**1^{st}: 0.64 V; 2^{nd} : 1.00 V vs Fc/Fc^+**	**93% capacity for 300 cycles (0.6 M)**	**11.0 Wh /L**
8[16]	1.19 V vs Fc/Fc^+	74% capacity for 100 cycles (0.05 M)	1.00 Wh /L
9[17]	1^{st}: 0.60 V; 2^{nd} : 1.20 V vs Fc/Fc^+	80% capacity for 250 cycles (0.03 M)	0.50 W h/L
10[18]	1.33 V vs Fc/Fc^+	13% capacity for 30 cycles (0.05 M)	1.65 W h/L

VI. Computational Methods

Conformational Analysis

Conformational searches were performed on the substrates using Macromodel version 11.7 with the OPLS3 force field.[19,20] Conformers within 2.5 kcal/mol of the lowest energy conformer were taken forward for DFT optimization.

DFT Properties

DFT calculations were undertaken using Gaussian 16 (Revision A.03).[21] Geometry optimization was carried out at the B3LYP/6-31+G(d,p)[22] and utilizing the GD3BJ empirical dispersion correction, as implemented in Gaussian 16 (Revision A.03). All ground states (zero imaginary frequencies) were verified as stationary points by frequency analysis. Optimized structures were visualized using CYLview.[23] NBO calculations were performed on the optimized geometry of most stable conformers at the uM06/def2tzvp level of theory using NBO 3.1. [24] HOMOs were visualized with Avogadro 1.2.0 using an isosurface value of 0.02. [25]

Parameter Collection

Parameters were then collected using Python scripts, similarly to previous reports from the Sigman lab.[26] Boltzmann-weighting of the properties was carried out using all of the computed conformers within 2.5 kcal/mol of the most stable conformer.

Geometry Data

The following data are Boltzmann averaged values from a conformational ensemble as described above. **SNDAC$^+$ angle** refers to the angle created by the phenothiazine sulfur (10), phenothiazine nitrogen (5), and the connecting carbon (11). **DAC$^+$ twist** refers to the dihedral angle created by carbon 13, nitrogen 5, carbon 11, and carbon 12. Though consistent atom selection was used to define these angles, depending on conformation, **DAC$^+$ twist** was either acute or obtuse. To normalize for comparison, when an obtuse value was obtained (>90°), the supplementary angle (180° – obtuse angle) was used as the corrected value of **DAC$^+$ twist**. These parameters are visualized on a +1 charged species of **4-Me** as an example below.

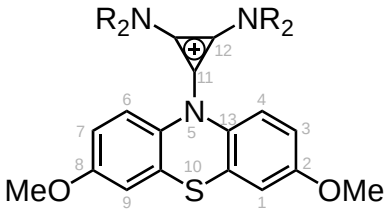

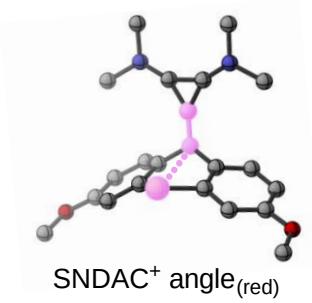

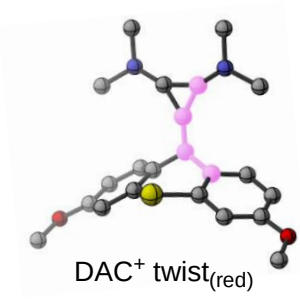

Selected Geometric Properties of Electrolytes in +1, +2, and +3 Oxidation State

	+1 Charge (Starting Material)		+2 Charge (First Oxidation)		+3 Charge (Second Oxidation)	
Compound	**SNDAC Angle**	**DAC Twist**	**SNDAC Angle**	**DAC Twist**	**SNDAC Angle**	**DAC Twist**
4-Me	107.2	17.7	174.3	45.8	179.9	59.3
4-Et	104.5	18.5	170.1	47.5	179.5	59.0
4-nPr	104.5	16.7	167.4	45.8	179.4	59.7
4-iPr	98.5	16.7	175.0	87.2	179.1	81.9
4-EtBu	102.7	17.9	167.3	46.8	179.9	64.6
4-Py	112.3	14.5	170.4	42.7	179.6	56.5
4-PIP	101.8	17.9	175.0	46.8	179.9	54.3
4-DMPP	143.2	27.2	179.9	54.7	179.4	75.7

Change in Selected Geometric Properties of Electrolytes from +1 to +2, and +2 to +3 Oxidation State

	+1 to +2 Charge (First Oxidation)		+2 to +3 Charge (Second Oxidation)	
Compound	**ΔSNDAC Angle**	**ΔDAC Twist**	**ΔSNDAC Angle**	**ΔDAC Twist**
4-Me	67.1	28.2	5.6	13.5
4-Et	65.6	29.0	9.3	11.6
4-nPr	62.9	29.2	12.0	13.9
4-iPr	76.5	70.5	4.1	-5.3
4-EtBu	64.6	28.9	12.6	17.8
4-Py	58.0	28.2	9.3	13.8
4-PIP	73.3	28.9	4.8	7.5

4-DMPP	34.3	27.5	1.9	21.0

Though **4-DMPP** technically contains an isopropyl moiety, the contribution of this group to steric bulk is much less than our initial intuition tells us. This can be seen computationally above, as the Boltzmann averaged ΔSNDAC Angle and ΔDAC Twist values (for both oxidations) for **4-DMPP** fall in line with the other compounds (rather than with **4-iPr**). These values are a direct reflection of the steric bulk that inhibits rotation about the N-DAC bond. Thus, it appears that despite the similar 2D topology of **4-DMPP** and **4-iPr**, when considered conformationally **4-DMPP** does not contribute sterically to induce the geometric change that is implicated as a differentiating factor in the 1st oxidation of the molecules.

Reference

[1] V. A. Chiykowski, B. Lam, C. Du, C. P. Berlinguette, *Chem. Commun.* **2017**, *53*, 2367.

[2] M. Kuroboshi, T. Yamamoto, H. Tanaka, *Synlett* **2013**, *24*, 197.

[3] Y. Jiang, J. L. Freyer, P. Cotanda, S. D. Brucks, K. L. Killops, J. S. Bandar, C. Torsitano, N. P. Balsara, T. H. Lambert, L. M. Campos, *Nature Communications* **2015**, *6*, 5950.

[4] K. H. Hendriks, S. G. Robinson, M. N. Braten, C. S. Sevov, B. A. Helms, M. S. Sigman, S. D. Minteer, M. S. Sanford, *ACS Cent. Sci.* **2018**, *4*, 189.

[5] Z. M. Strater, M. Rauch, S. Jockusch, T. H. Lambert, *Angewandte Chemie International Edition* **2019**, *58*, 8049.

[6] S. G. Robinson, Y. Yan, K. H. Hendriks, M. S. Sanford, M. S. Sigman, *J. Am. Chem. Soc.* **2019**, *141*, 10171.

[7] J. D. Milshtein, A. P. Kaur, M. D. Casselman, J. A. Kowalski, S. Modekrutti, P. L. Zhang, N. Harsha Attanayake, C. F. Elliott, S. R. Parkin, C. Risko, F. R. Brushett, S. A. Odom, *Energy Environ. Sci.* **2016**, *9*, 3531.

[8] A. A. A. Aljabali, J. E. Barclay, J. N. Butt, G. P. Lomonossoff, D. J. Evans, *Dalton Trans.* **2010**, *39*, 7569.

[9] R. S. Nicholson, *Anal. Chem.* **1965**, *37*, 1351.

[10] C. Zhang, Z. Niu, Y. Ding, L. Zhang, Y. Zhou, X. Guo, X. Zhang, Y. Zhao, G. Yu, *Chem* **2018**, *4*, 2814.

[11] W. Duan, R. S. Vemuri, J. D. Milshtein, S. Laramie, R. D. Dmello, J. Huang, L. Zhang, D. Hu, M. Vijayakumar, W. Wang, J. Liu, R. M. Darling, L. Thompson, K. Smith, J. S. Moore, F. R. Brushett, X. Wei, *J. Mater. Chem. A* **2016**, *4*, 5448.

[12] N. Harsha Attanayake, Z. Liang, Y. Wang, A. Preet Kaur, S. R. Parkin, J. K. Mobley, R. H. Ewoldt, J. Landon, S. A. Odom, *Materials Advances* **2021**, *2*, 1390.

[13] G. Kwon, S. Lee, J. Hwang, H.-S. Shim, B. Lee, M. H. Lee, Y. Ko, S.-K. Jung, K. Ku, J. Hong, K. Kang, *Joule* **2018**, *2*, 1771.

[14] W. Duan, J. Huang, J. A. Kowalski, I. A. Shkrob, M. Vijayakumar, E. Walter, B. Pan, Z. Yang, J. D. Milshtein, B. Li, C. Liao, Z. Zhang, W. Wang, J. Liu, J. S. Moore, F. R. Brushett, L. Zhang, X. Wei, *ACS Energy Lett.* **2017**, *2*, 1156.

[15] A. Shrestha, K. H. Hendriks, M. S. Sigman, S. D. Minteer, M. S. Sanford, *Chemistry – A European Journal* **2020**, *26*, 5369.

[16] Y. Yan, T. P. Vaid, M. S. Sanford, *J. Am. Chem. Soc.* **2020**, *142*, 17564.

[17] Y. Yan, S. G. Robinson, T. P. Vaid, M. S. Sigman, M. S. Sanford, *J. Am. Chem. Soc.* **2021**, *143*, 13450.

[18] Y. Yan, S. G. Robinson, M. S. Sigman, M. S. Sanford, *J. Am. Chem. Soc.* **2019**, *141*, 15301.

[19] E. Harder, W. Damm, J. Maple, C. Wu, M. Reboul, J. Y. Xiang, L. Wang, D. Lupyan, M. K. Dahlgren, J. L. Knight, J. W. Kaus, D. S. Cerutti, G. Krilov, W. L. Jorgensen, R. Abel, R. A. Friesner, *J Chem Theory Comput* **2016**, *12*, 281.

[20] K. Roos, C. Wu, W. Damm, M. Reboul, J. M. Stevenson, C. Lu, M. K. Dahlgren, S. Mondal, W. Chen, L. Wang, R. Abel, R. A. Friesner, E. D. Harder, *J. Chem. Theory Comput.* **2019**, *15*, 1863.

[21] M. J. Frisch, G. W. Trucks, H. B. Schlegel, G. E. Scuseria, M. A. Robb, J. R. Cheeseman, G. Scalmani, V. Barone, G. A. Petersson, H. Nakatsuji, X. Li, M. Caricato,

A. V. Marenich, J. Bloino, B. G. Janesko, R. Gomperts, B. Mennucci, H. P. Hratchian, J. V. Ortiz, A. F. Izmaylov, J. L. Sonnenberg, Williams, F. Ding, F. Lipparini, F. Egidi, J. Goings, B. Peng, A. Petrone, T. Henderson, D. Ranasinghe, V. G. Zakrzewski, J. Gao, N. Rega, G. Zheng, W. Liang, M. Hada, M. Ehara, K. Toyota, R. Fukuda, J. Hasegawa, M. Ishida, T. Nakajima, Y. Honda, O. Kitao, H. Nakai, T. Vreven, K. Throssell, J. A. Montgomery Jr., J. E. Peralta, F. Ogliaro, M. J. Bearpark, J. J. Heyd, E. N. Brothers, K. N. Kudin, V. N. Staroverov, T. A. Keith, R. Kobayashi, J. Normand, K. Raghavachari, A. P. Rendell, J. C. Burant, S. S. Iyengar, J. Tomasi, M. Cossi, J. M. Millam, M. Klene, C. Adamo, R. Cammi, J. W. Ochterski, R. L. Martin, K. Morokuma, O. Farkas, J. B. Foresman, D. J. Fox, *Gaussian 16 Rev. B.01*, Wallingford, CT, **2016**.

[22] A. D. McLean, G. S. Chandler, *J. Chem. Phys.* **1980**, *72*, 5639.

[23] C. Legault, *CYLview 1.0b*, Université De Sherbrooke, **2009**.

[24] E. Glendening, A. Reed, F. Carpenter, *NBO Version 3.1.*, **n.d.**

[25] M. D. Hanwell, D. E. Curtis, D. C. Lonie, T. Vandermeersch, E. Zurek, G. R. Hutchison, *Journal of Cheminformatics* **2012**, *4*, 17.

[26] S. Zhao, T. Gensch, B. Murray, Z. L. Niemeyer, M. S. Sigman, M. R. Biscoe, *Science* **2018**, *362*, 670.